Original Article

MOLECULAR METABOLISM

Intrinsic cardiorespiratory fitness modulates clinical and molecular response to caloric restriction

Johanna Y. Fleischman [1,8], Nathan R. Qi [1,2,3,8], Mary K. Treutelaar [2], Steven L. Britton [1,4], Lauren G. Koch [5], Jun Z. Li [6,7], Charles F. Burant [1,2,*]

ABSTRACT

Objective: Caloric restriction (CR) is one extrinsic intervention that can improve metabolic health, and it shares many phenotypical parallels with intrinsic high cardiorespiratory fitness (CRF), including reduced adiposity, increased cardiometabolic health, and increased longevity. CRF is a highly heritable trait in humans and has been established in a genetic rat model selectively bred for high (HCR) and low (LCR) CRF, in which the HCR live longer and have reduced body weight compared to LCR. This study addresses whether the inherited high CRF phenotype occurs through similar mechanisms by which CR promotes health and longevity.

Methods: We compared HCR and LCR male rats fed *ad libitum* (AL) or calorically restricted (CR) for multiple physiological, metabolic, and molecular traits, including running capacity at 2, 8, and 12 months; per-hour metabolic cage activity over daily cycles at 6 and 12 months; and plasma lipidomics, liver and muscle transcriptomics, and body composition after 12 months of treatment.

Results: LCR-CR developed a physiological profile that mirrors the high-CRF phenotype in HCR-AL, including reduced adiposity and increased insulin sensitivity. HCR show higher spontaneous activity than LCR. Temporal modeling of hourly energy expenditure (EE) dynamics during the day, adjusted for body weight and hourly activity levels, suggest that CR has an EE-suppressing effect, and high-CRF has an EE-enhancing effect. Pathway analysis of gene transcripts indicates that HCR and LCR both show a response to CR that is similar in the muscle and different in the liver.

Conclusions: CR provides LCR a health-associated positive effect on physiological parameters that strongly resemble HCR. Analysis of whole-body EE and transcriptomics suggests that HCR and LCR show line-dependent responses to CR that may be accreditable to difference in genetic makeup. The results do not preclude the possibility that CRF and CR pathways may converge.

Keywords Caloric restriction; Cardiorespiratory fitness; Mitochondria; Metabolism; Muscle

1. INTRODUCTION

Caloric restriction (CR) increases metabolic health and longevity across multiple species, including worms [1], flies [2], mice [3], and rats [4], the latter dating back to one of the first CR and longevity study published in 1935. Studies in monkeys also show improved metabolic health in CR over *ad libitum* (AL) feeding [5]. While longevity outcomes are difficult to examine in humans, CR has been shown to decrease body weight, reduce heart disease risk, increase insulin sensitivity [6], and optimize immunity [7]. One possible mechanism for these changes is reduced metabolic rate [8], although the universality of the effect is debated [9].

Cardiorespiratory fitness (CRF) is an intrinsic physiological trait that is also associated with longevity [13]. CRF, defined as the ability of the circulatory and respiratory systems to supply oxygen to skeletal muscles during sustained exercise, is routinely measured by maximal oxygen uptake (VO_2max) during a graded exercise test. CRF is a highly heritable trait in humans [10] and, importantly, inherited high CRF phenotypes mirror the CR-induced phenotypes, including lower adiposity [11], higher cardiometabolic health [12], and greater longevity [13]. As such, a key question in the field is whether CR "phenocopies" the intrinsic high-CRF characteristics via similar, overlapping, or distinct mechanisms.

[1]Department of Molecular and Integrative Physiology, University of Michigan, Ann Arbor, MI, USA [2]Department of Internal Medicine, University of Michigan, Ann Arbor, MI, USA [3]Michigan Mouse Metabolic Phenotyping Center, University of Michigan, Ann Arbor, MI, USA [4]Department of Anesthesiology, University of Michigan, Ann Arbor, MI, USA [5]Department of Physiology and Pharmacology, The University of Toledo, Toledo, OH, USA [6]Department of Human Genetics, University of Michigan, Ann Arbor, MI, USA [7]Department of Computational Medicine and Bioinformatics, University of Michigan, Ann Arbor, MI, USA

[8] Co-first author.

*Corresponding author. 6309 Brehm Tower, 1000 Wall Street, Room 6309, Ann Arbor, MI 48105-5714, USA. E-mail: burantc@med.umich.edu (C.F. Burant).

Abbreviations: CRF, cardiorespiratory fitness; HCR, high-capacity runner; LCR, low-capacity runner; CR, caloric restriction & calorically restricted; AL, ad libitum; EE, energy expenditure; FAO, fatty acid oxidation; BW, body weight; OR, odds ratio

Received October 25, 2022 • Revision received December 21, 2022 • Accepted January 5, 2023 • Available online 12 January 2023

https://doi.org/10.1016/j.molmet.2023.101668

We have been characterizing an established rat model selectively bred from a genetically heterogeneous stock (N:NIH) to generate a high capacity runner (HCR) line and low capacity runner (LCR) line in a manner that maintains genetic heterogeneity [14–16]. HCR exhibit high CRF phenotypes when compared to LCR, including lower body weight even after adjusting for food consumption and exercise [14,17] greater protection from multiple diseases [18,19], and longer lifespan [20]. Significant body weight differences between lines developed early in the selection process despite similar net food intake in both lines [14]. These lines present us a unique opportunity to compare and contrast the endogenous CRF phenotypes with those induced by CR over a diverse set of molecular, metabolic, and physiological traits, including dynamic traits that are particularly difficult to measure in humans.

Suggested mechanisms for the intrinsic differences in weight gain in the HCR and LCR include heat dissipation and efficiency of skeletal muscle mitochondria coupling [17]. Adaptations in whole-body energy expenditure (EE) and fuel utilization have been observed both with CR [21–23] and with inherited CRF [16], but a major difficulty linking food intake, weight gain, and EE is that these variables are closely entwined with spontaneous activity, which has been implicated in CRF [24] and controversially with CR [21]. Older studies of CR in rats reported decreases in EE and heat production with CR [21,22] but these studies have not accounted for the variation due to spontaneous activity. In this study, we systematically investigate these factors by performing a dynamic analysis of EE and other metabolic features in each line under CR. Daily body weight, hourly oxygen consumption, and hourly activity data were observed such that the innate contributions of genetic fitness and CR on whole-body metabolism could be calculated in a body weight- and activity-independent manner.

2. METHODS

2.1. Overview of study design and group assignment

Our study adopted a 2 × 2 factorial design to examine the effects of two binary factors: genetic line (HCR and LCR) and feeding treatment (al libitum, AL; or calorically restricted to 60% of AL calories, CR) over the course of 12 months starting from weaning (4 weeks old) (Figure 1A). Twenty-four male rats of each line (LCR and HCR of generation 22 at 3–4 weeks of age) were assigned to AL and CR groups. For weight matching, rats within each line were ranked by body weight, and successive pairs were alternatively assigned to AL or CR. In this manner, each CR cage had a weight-matched AL cage from which food quantities were calculated. In the final assignment of 48 rats to 12 per group, AL and CR groups did not differ in starting body weight (Fig. S1A) in either line.

2.2. Animal care and measurements of body weight and food intake

The AL groups were fed *ad libitum* with the NIH31 diet, and the CR groups were provided with the NIH31/NIA diet fortified with extra vitamins. At 4–5 weeks old, the CR groups received a gradually reduced daily allotment of food over 4 weeks, to 90%, 80%, 70%, and 60% (w/w) per week of the daily average amount consumed by the matched AL cage of the same line during the preceding week. CR groups were subsequently maintained at 60% of food intake of the weight rank-matched AL rats throughout the experiment (12 months). Food for CR groups was provided daily between 4:30pm to 5:00pm. Body weight and food intake were measured weekly at the same time of the same day. All animals were housed in a pathogen-free environment with constant room temperature (20–22 °C) and relative humidity (40–50%) and a 6:00pm-6:00am dark–light cycle. Water was provided AL for all animals. All procedures were approved by the University of Michigan Animal Care and Use Committee.

2.3. Endurance running capacity

Endurance running capacity of each rat was tested using an incremental speed protocol as described previously [14] with some modifications. Briefly, rats were introduced to the treadmill (model Exer-4; Columbus Instruments) in the week before the initial test by running for 5 min at a speed of 10 m/min on a 15° slope on three consecutive days (Monday, Wednesday, and Friday). Subsequently, rats were evaluated for maximal endurance running capacity at 2, 8, and 12 months of age. The test was performed in the morning between 9am and 12pm on three days (Monday, Wednesday, and Friday), and each daily endurance trial was performed at a constant slope of 15° with the starting velocity at 10 m/min. Treadmill velocity was increased by 1 m/min every 2 min and each rat was run until exhausted. Exhaustion was operationally defined as the third time a rat could no longer keep pace with the treadmill and remained on the shock grid for 2 s rather than run. Of the three trials, the single best daily run calculated in distance (meters) and work (Joule) was used as the estimate of endurance running capacity. Work was calculated using the following equation, where 0.2588 m is the vertical distance run per meter:

$$Work = \frac{Body\ weight_{grams}}{1000} \times Distance_{meters} \times 0.2588 \times g$$

2.4. Body composition, temperature, blood, and tissue collection and analysis

Body fat and lean mass were estimated using an NMR-based analyzer (Minispec LF90II, Bruker Optics) under conscious conditions after 10 months of treatment. Core body temperature was collected after 6 and 10 months of treatment using a rectal temperature probe. After 12 months of treatment, food was removed from AL groups at 8:00 am while CR groups were kept on their normal feeding schedule. Rats of all groups were randomly divided and sacrificed under ketamine anesthesia (60–80 mg/kg, i.p.) either at 3:00pm-5:00pm (fasted) or 5:00pm-7:00pm (fed). Rats of CR groups were provided with their daily allotments and the food was usually consumed in 30 min, whereas all AL rats were fed *ad libitum* and the food was removed after 2 h of feeding. Trunk blood was collected, and the plasma was separated and stored in −80 °C. The soleus, EDL, tibialis, heart, liver, kidney, epididymal adipose tissue, and brown adipose tissue were weighed, immediately frozen in liquid nitrogen, and stored in −80 °C for subsequent analyses. For analysis of body composition, temperature, organ weights, blood chemistry, and running capacity, the group means and standard errors ($n = 12$) were calculated and reported (Table S1). Main line effects, main treatment effects, and interaction effects were determined to be significant for $p < 0.05$ using two-way ANOVA regression in R (*lm*).

2.5. Indirect calorimetry measurement

We collected three types of physiologic data from metabolic cages: VO_2 consumption, VCO_2 production, and spontaneous activity. Experiments were performed after 6 and 12 months of CR treatment using an integrated open-circuit calorimetry system (CLAMS, Columbus Instruments) equipped with an infrared photo–beam activity device for monitoring spontaneous activity while animals were housed in the recording chambers. Body weight was measured before entering the cage and after exiting the cage. VO_2 and VCO_2 were sampled sequentially in each chamber for 5 s in a 10 min interval and the motor activity was recorded every second in X and Z dimensions

simultaneously for 48–72 h. During this time, animals were provided with food on the cage floor and with water through the drinking devices located inside the measuring chambers. CR animals were fed at the same time as they were fed in their home cages. The air flow rate through the chambers was adjusted to a level to keep the oxygen differential around 0.3% at resting conditions. Respiratory exchange ratio (RER) was calculated as VCO_2/VO_2. Whole-body fat oxidation, glucose oxidation, and energy expenditure (EE) rates were estimated from VCO_2 and VO_2 [25–28].

2.6. Data normalization by weight and by activity

Hourly recordings over five 24-hr days were collected from the metabolic cages: 2 consecutive days at 6 months of CR and 3 consecutive days at 12 months of CR. Data from metabolic cages were provided as units per hour. In addition to EE, VO_2, fat oxidation, and glucose oxidation ("Variable") were subjected to the same two-step adjustment described below.

EE is known to depend on body weight, so we calculated the body weight-adjusted values by linear regression against body weight over the 48 animals. Beta estimates were generated independently for each day (d, n = 5) using the body weights collected on the first day of recording for each month (m, n = 2):

$$Variable_{i,d,h} \sim BW_{i,m}$$

where BW = body weight, i = animal, and h = hour. Subsequently, body weight-adjusted metabolic cage values were generated:

$$Variable_{BW_{adj},i,d,h} = Variable_{raw,i,d,h} + beta_d\left(\overline{BW_m} - BW_{i,m}\right)$$

Next, as EE varied with activity on an hourly basis, we estimated the linear relationship between hourly body weight-adjusted EE and activity using a linear regression model over the 24 h and is performed separately for each of 48 animals (i) and each of 5 days (d). Beta estimates were generated for each day and each animal (Fig. S4):

$$Variable_{BW_{adj},i,d,h} \sim Activity_{i,d,h}$$

Subsequently, activity-adjusted metabolic cage values were generated by using the regression result, centered on the mean activity level of all 48 animals across all 24 h on each of the 5 days:

$$Variable_{BW+Activity_{adj},i,d,h} = Variable_{BW_{adj},i,d,h} + beta_{i,d}\left(\overline{Activity_d} - Activity_{i,d,h}\right)$$

Adjusting the activity to the daily global activity mean reduces the variation due to both (1) activity differences throughout hours of the day, and (2) activity differences between animals. The body weight-adjusted values showed high correlations between days and between the animals within Line-Treatment groups (Figs. S6–S8). This observation allowed us to combine the repeated daily measurements for subsequent analysis by averaging the adjusted values for all animals and all days for each Line-Treatment group.

2.7. Gene expression

RNA was isolated from snap-frozen whole gastrocnemius and liver tissues, and mRNA levels were estimated using an Illumina Gene Expression BeadChip Array. The array generated data for 22,523 genes that were normalized by the University of Michigan Advanced Genomics Core using cubic spline normalization to correct for non-linear relationships between samples in log space. The intensity distribution was divided into a group of quantiles consisting of a similar number of gene intensities and adjusted to match intensities from the virtual array. Intensities were then log2 scaled.

Differential gene expression data for both the liver and skeletal muscle was quantified in R using the *limma* package. Gene expression was normalized to the fed or fasted state (*removeBatchEffect*) for muscle. The liver data was only assessed from fasted animals. To determine differential gene expression, each gene was fitted with a linear model (*lmFit*) and the standard errors were determined using a simple empirical Bayes model (*eBayes*). Main effects were quantified by group using the model $Gene \sim Line + Treatment$ where the *Line* variable contained 2 factors corresponding to HCR and LCR, and the *Treatment* variable contained 2 factors corresponding to CR and AL. Differential gene expression for main effects were determined using 2 contrasts: HCR—LCR, and CR—AL. Interaction term effects were quantified by group using the model $Gene \sim Line + Treatment + Line : Treatment$. Differential gene expression for interaction effects were determined using 4 contrasts: HCR.AL—LCR.AL, HCR.CR—LCR.CR, HCR.CR—HCR.AL, and LCR.CR—LCR.AL. Data for these 2 models were generated for liver and muscle, resulting in a total of 12 comparisons. P-values were FDR-adjusted using Benjamini-Hochberg (*p.adjust*). Pathway analysis was performed using p-values and LogFC in LRPath [29] filtering for KEGG pathways. LRpath recognized 12,592 gene IDs which contribute to results of the pathway analysis.

2.8. Lipidomics

Data was generated using liquid chromatography-mass spectrometry (LC-MS) with assistance from the Metabolomics Core at the University of Michigan. Positive-ion mode and negative-ion mode MS analyses were combined with repeat peaks removed. Metabolites with relative standard deviation (RSD) values > 0.4 in pooled control samples were removed. Six metabolites with unknown identities were removed. Remaining output data was normalized to the total summed peak area and log_2-transformed before subsequent analysis.

Lipid clusters were defined a priori (Table S4) based on lipid class, carbon chain length, and number of double bonds, as has been performed previously [30]. To determine cluster values, the normalized (mean = 0, standard deviation = 1) relative abundance of each lipid (l) within each cluster was multiplied by the absolute value of the loading (or rotation) factor from principal component 1 (R *prcomp*). These values were summed to generate a cluster value for each animal (i):

$$Lipid\ Cluster_i = \sum_l \left(Lipid_{i,l} * \left|Multiplier_{PC1}\right|_l\right)$$

The R *lm* function was used to determine the amount of variability in lipid clusters described by *Line*, *Treatment*, and the *State* (fed/fasted) and the *Treatment* : *Line* interaction. Each lipid cluster was normalized (mean = 0, standard deviation = 1) before linear regression analysis:

$$\widehat{Lipid\ Cluster}_i = \beta_0 + \beta_1 * State + \beta_2 * Treatment + \beta_3 * Line + \beta_4 * Treatment : Line$$

3. RESULTS

3.1. LCR physiology under CR reflects the intrinsic HCR phenotype

Food intake and body weight were tracked weekly; and rats were intermittently tested for running capacity, metabolic cage activity, and temperature (Figure 1A). Over 12 months, LCR gained more body weight than HCR for both AL and CR groups (Figure 1B) with a mean difference of 109.75 g between AL groups and 37.12 g between CR

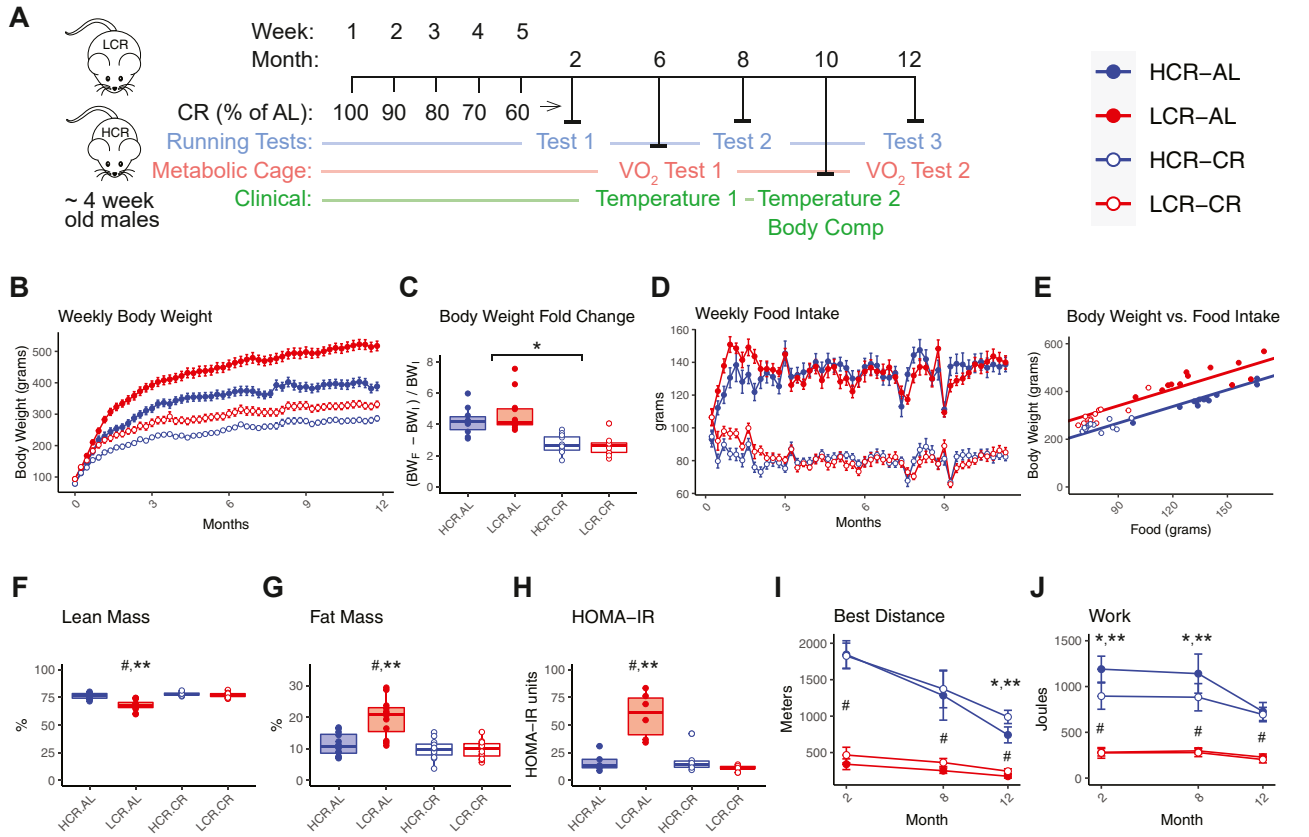

Figure 1: LCR physiology under CR reflects the HCR phenotype. Male HCR and LCR rats were fed ad lib (AL) or calorically restricted (CR) at 60% of ad lib calories for 12 months (A). Total body weight was calculated for each group for each week of study (B). Both CR groups gained less weight than their AL counterparts, although respective reduction in weight gain was not different between HCR and LCR (C). Food consumption was equivalent in HCR and LCR within AL and CR groups (D). Body weight (grams) is plotted as a linear function of food intake (grams) and Line for week 26 (halfway point) of the study to exemplify the distinct relationship between food intake and body weight in HCR and LCR (E). LCR-CR experienced a significant increase in % weight as lean mass (F), decrease in % weight as fat (G), and decrease in insulin resistance (H) over treatment period compared to LCR-AL. VO_2max tests are shown as best distance (I) and work generated over the best distance (J). Significance was determined using two-way ANOVA with interaction (R *lm*) and main line effects, main treatment effects, and interaction effects with p-values <0.05 are annotated. *#Main line effect, *Main caloric restriction effect, **Interaction effect; HCR = high capacity runner; LCR = low capacity runner; AL = ad libitum; CR = caloric restriction; Body Comp = Body composition; Test = VO_2max test; BW_I = initial body weight; BW_F = final body weight.*

groups ($p < 0.003$ for Line, Treatment, and Interaction effect, Table S1). The percent gain in weight (12-month over 0-month, Figure 1C) and net weekly food intake (Figure 1D) was significantly lower in both CR groups but did not differ between HCR and LCR (Table S1). Regression analysis of body weight after week 4 as a linear function of $\sim Week + Line + Food\ Intake$ ($R^2 = 0.84$) was significant for all variables ($\beta_{Week} = 3.1$, $\beta_{LCR} = 69.5$, $\beta_{Food} = 2.3$, $p < 0.001$, Figure 1E) with the line estimate supporting the previously reported finding that LCR weigh more than HCR despite equivalent food intake [17]. Bomb calorimetry data from the feces in a separate AL cohort did not show differences in fecal energy content between HCR and LCR (Fig. S1B) indicating that malabsorption does not contribute to lower relative body weight in the HCR.

CR was associated with a decrease in fat mass in LCR and eliminated fat mass percent differences seen in the lines under AL conditions (Figure 1F and G; $p < 0.001$ for Line and Interaction effect, Table S1). At baseline, LCR-AL had higher HOMA-IR, a measure of insulin sensitivity, than HCR-AL, and CR decreased HOMA-IR in the LCR but not the HCR (Figure 1H; $p < 0.001$ for Line and Interaction effect, Table S1) resulting in similar insulin sensitivity in HCR-AL, HCR-CR, and LCR-CR. The net muscle weights of soleus, tibialis, and heart showed a significant decrease with CR ($p < 0.001$ for Treatment effect, Table S1) but no significant difference between lines. When normalized to body weight, HCR muscle weights were higher than LCR for soleus, EDL, tibialis, and heart ($p < 0.001$ for Line effect, Table S1) but only normalized heart weight was higher with CR treatment ($p < 0.001$ for Treatment effect, Table S1) suggesting greater preservation of heart muscle compared to skeletal muscle under CR.

Animals completed three VO_2max running tests at 2, 8, and 12 months of age. HCR had a higher running capacity (which is directly related to VO_2max [20]) than LCR in both AL and CR conditions (Figure 1I; $p < 0.001$ for Line effect, Table S1). CR slightly increased running distances in both lines, which was only significant for HCR at 12 months (Figure 1I; $p < 0.001$ for Interaction effect, Table S1). To account for the fact that weight differs between the lines, we also calculated Work as a function of body weight times vertical running displacement (Figure 1J) which showed equivalent work capacities in LCR-AL and LCR-CR but lower work capacities in the HCR-CR compared to HCR-AL. The

comparison of Work suggests that the slightly longer running distances of LCR-CR than LCR-AL could be attributed to the lower body weight of the former. In contrast, the HCR-AL and HCR-CR ran equivalent distances at the 2- and 8-month timepoints (Figure 1I) which is likely a function of their selection for maximal fitness, which was not perturbed by CR. Similarly, the lower work capacity in HCR-CR reflects the lower body weights in HCR-CR compared to HCR-AL.

Of the physiological measures described above, HCR-AL and HCR-CR are similar, and they differ from LCR-AL, especially regarding body composition and insulin sensitivity. Importantly, LCR-CR resembles both HCR groups, showing that LCR has "room to change" with 1-year of CR treatment, whereas HCR has little room. However, the HCR-CR do have reduced body weight gain compared to HCR-AL, indicating that CR does have an independent effect from the genetic selection for intrinsic fitness.

3.2. The resting and activity-dependent components of energy expenditure can be separated by adjusting for activity level across hours of the day

We next performed a detailed analysis of whole-body energy balance in each line following AL and CR to further explore the non-overlapping nature of the endogenous HCR phenotype and CR-induced changes. A systemic comparison of innate energy expenditure (EE) between lines and treatments must account for the body weight differences between animals [31] and physical activity differences between animals and across hours of the day [32]. Past studies in HCR and LCR have underscored the importance of body weight and activity on EE [33] and show higher spontaneous activity in HCR rats [34,35] although some studies have shown negligible differences between lines [36]. In this evaluation, HCR showed higher activity levels compared to LCR ($p < 0.01$ each day for Line effect, Figure 2A) with greatest contributions in the dark (active) cycle (Fig. S2F). This variability in physical activity across 24 h and between lines supported the requisite to adjust for activity in a dynamic analysis. We first quantified the relationship between body weight and EE and then between cage activity and body weight-adjusted EE using data from the metabolic cages (Fig. S2, Table S2). The result allowed us to compare baseline EE dynamics over the 24-hr day under the assumption that body weight and activity levels are consistent for all animals across all groups. This two-step adjusted EE, hereafter referred to as "innate" EE, aims to capture the unmeasured thermic effect of food and residual differences in EE. Several other variables were not considered in this analysis, because the animals (1) were all male, (2) were age matched, (3) showed no difference in thyroid hormones levels (free T3 and free T4) (Table S1); and (4) showed a lower brown adipose tissue (BAT) weight in HCR than LCR (Table S1) but no differences in core body temperature between lines (Fig. S1C). The raw data was first stratified by the 4 groups (12 animals each) and the 5 days (hourly metabolic cage data was collected for 2 days at 6 months and 3 days at 12 months) (Figs. S3A and S3B). For each of the 5 days, EE values were regressed against the 48 animals' body weight of that day. The slope of the regression model captures the dependency of each animal's EE values on its body weight and was used to calculate a body weight-adjusted EE value (Fig. S3C), where the 24-hourly values for each animal receives the same adjustment. In the next step, body weight-adjusted EE values were adjusted for hourly physical activity using the regression of body weight-adjusted EE over 24 h against the corresponding hourly levels of activity. This is done for each of the 48 animals and each of the 5 days, to form 240 independent regression analyses that account for each animals' specific relationship between activity levels and EE. In each model, body weight-adjusted EE values correlated strongly with raw cage activity counts in each animal (Fig. S4). As with the body weight-adjustment, we used the regression slopes from the 240 series of data to obtain the activity-adjusted EE for each animal (Fig. S3D). The activity-adjusted EE accounted for variability in activity across all hours of the day, as well between different animals, by centering the data over the global activity mean of all animals and all hours for each of the 5 days.

This analysis results in a measure of EE over 24 h in each Line-Treatment group that assumes an equivalent body weight and activity level. In addition to EE, we have measured fat oxidation, which had the same data organization and was subjected to the same two-step adjustment as EE. The hourly data for each of the 5 days and each of the 12 animals correlated significantly within each Line-Treatment group for raw activity counts (Fig. S6), body weight-adjusted EE (Fig. S7), and body weight-adjusted fat oxidation (Fig. S8) for which reason the 5-days of data for each Line-Treatment group was averaged to analyze hourly trends in energy utilization.

3.3. High CRF is associated with increased body weight-adjusted energy expenditure and CR promotes fatty acid oxidation

Over the 24-hour day, grossly measured EE showed a dynamic pattern, with a marked rise near the feeding time (Figure 2B, Fig. S3A). The rise in EE started before feeding, presumably reflecting increased activity in anticipation of the regularly scheduled feeding. The four Line-Treatment groups showed strong differences in both the absolute levels and the dynamic hourly patterns, in which the AL rats generally had a higher EE than CR, and to a lesser extent, that LCR had higher EE than HCR. As body weight contributes to the absolute levels of EE [17], we first examined the body weight-adjusted EE (Figure 2C, Fig. S3C), which reduced the differences between Lines and between Treatment, although a prominent rise near feeding time was still observed. Subtle differences in dynamic patterns were also notable across the 4 groups, especially for HCR-AL, which had a moderately higher body weight-adjusted EE than other groups before feeding and much higher after feeding.

Adjusting body weight-adjusted EE by hourly activity led to an estimated innate EE, which showed more moderate dynamic patterns across the 24 h (Figure 2D, Fig. S3D). The sharp increase in EE around feeding time was reduced after adjusting for activity, indicating that most of the observed late-afternoon peak in EE was due to the heightened physical activity around the same time, which can also be readily observed by comparing the mean hourly Activity levels of each group (Figure 2E) to the mean hourly body weight-adjusted EE of each group (Figure 2F). The innate EE, which captures thermogenesis and the thermic effect of food digestion, shows a rise prior to feeding and peaks following feeding (Figure 2D). AL animals have higher post-prandial innate EE compared to CR, which is likely due, in part, to the thermic effect of food. CR animals show a similar rise, but a rapid decline, which likely reflects the rapid consumption of food. Between lines in each AL and CR group, HCR have higher innate EE than LCR. Two-way ANOVA on the AUCs of 24-hour innate EE supports these findings ($p < 0.001$ for Treatment effect and $p = 0.082$ for Line effect) but indicates that the EE-suppressing effect of CR ($\beta_{Treatment} = -2.9$) is more significant than the EE-enhancing effect of being an HCR ($\beta_{HCR} = 1.3$). Tukey post-hoc analysis on the interaction term suggests that HCR ($\beta_{HCR:CR} = -3.5$, $p = 0.008$) experience a more robust CR-suppressing effect than LCR ($\beta_{LCR:CR} = -2.3$, $p = 0.15$).

Whole-body fatty acid oxidation (FAO) was estimated from VCO_2 and VO_2 [27], and as with EE, was regression-normalized to body weight for analysis. Adjusting FAO for activity did not significantly affect values (Table S2). As expected [37], CR groups exhibited increased FAO compared to AL groups, which presented in a diurnal pattern with an

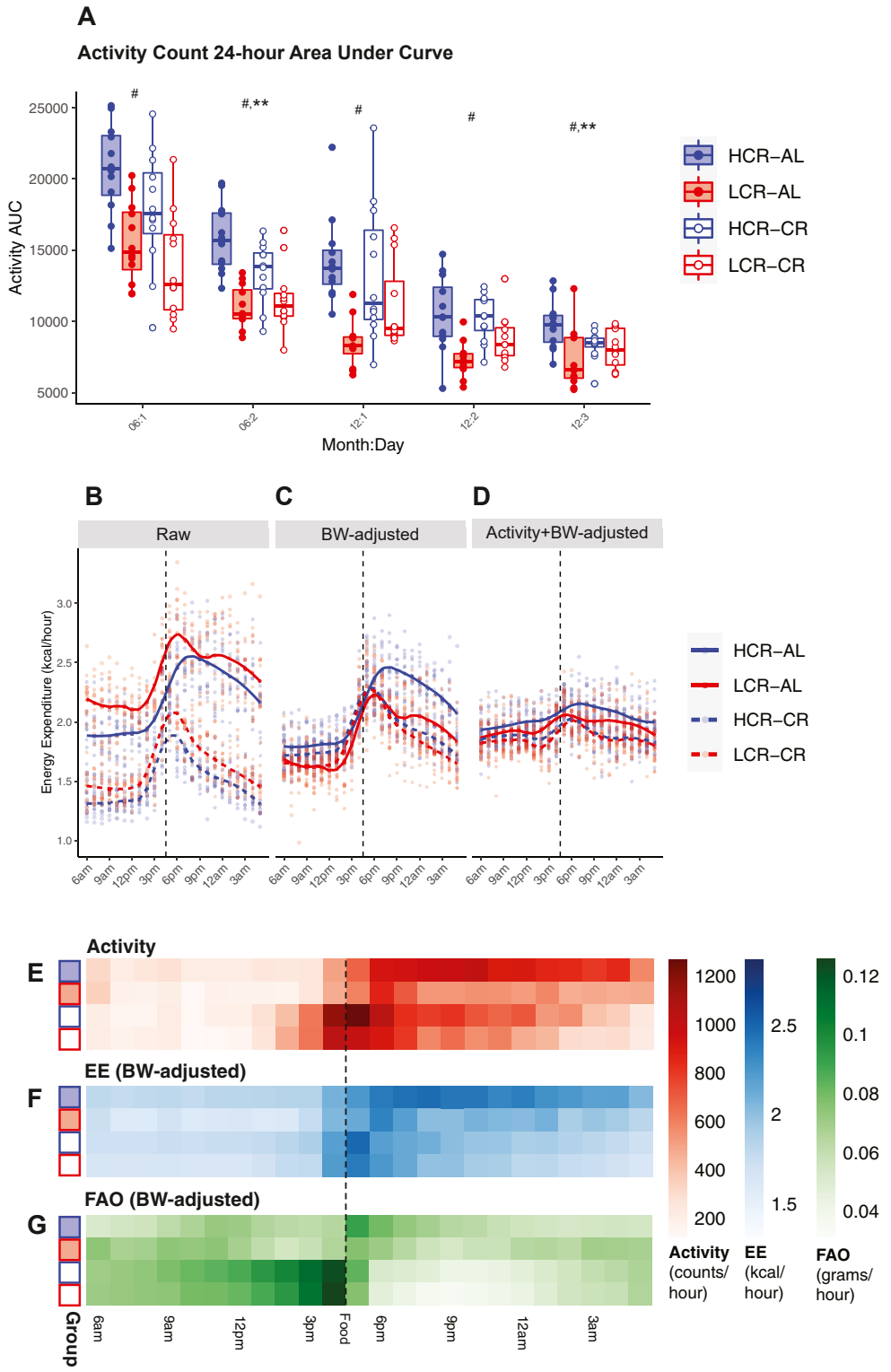

Figure 2: High-CRF is associated with increased body weight-adjusted energy expenditure and CR promotes fatty acid oxidation. HCR and LCR were placed in metabolic cages at 6 months and 12 months of CR to measure whole-body VO_2 and VCO_2 and cage activity. AUC measurements of hourly cage activity means (beam breaks), separated by Line-Treatment groups each day, were derived from Fig. S2F (A). Average energy expenditure (EE) over 5 days for each hour is visualized as a LOESS curve for raw data (B), body weight-adjusted data (C), and body weight- and activity-adjusted data (D) using linear regression. Five-day average of activity counts (E), body weight-adjusted EE (F), and body weight-adjusted fatty acid oxidation (G) are compared to illustrate synchronized diurnal patterns. Dotted lines represent feeding time. For 2A, significance was determined using two-way ANOVA with interaction (R *lm*) for each day, and main line effects, main treatment effects, and interaction effects with p-values <0.05 are annotated. $^{\#}$*Main line effect,* **Main caloric restriction effect,* ***Interaction effect; HCR = high capacity runner; LCR = low capacity runner; AL = ad libitum; CR = caloric restriction; BW = body weight; EE = energy expenditure; FAO = fatty acid oxidation.*

acute increase before feeding time (Figure 2G). There were minimal significant differences in FAO between HCR and LCR in either AL or CR groups, although significant variability within the AL groups was observed (Figs. S8A and S8C). In contrast, the 24-hour pattern in FAO was highly correlated between animals in CR groups (Figs. S8B and S8D) due to synchronized increase in FAO at the end of the fasting period.

3.4. CR-associated regulation of gene expression in HCR and LCR is tissue dependent

To further investigate the line-dependent responses to CR, gene microarray data was collected from skeletal muscle and liver tissues harvested at the 12-month timepoint. Principal Component Analysis (PCA) on all muscle genes showed that line, but not CR treatment, separates in PC space across both PC1 (18.3%) and PC2 (13.3%) (Figure 3A). This is supported by the number of differential genes expressed by line (1913) which was greater than CR treatment (638) using a main effect model (Fig. S9A). To better characterize the genes altered by CR, CR genes (Fig. S9A) were plotted in PC space, which showed that these genes are already differentially expressed at baseline in HCR and LCR in muscle (Figure 3B and C). However, only 118 of these 638 CR genes (FDR <0.05) were significantly differentially expressed between HCR and LCR (Fig. S9A) suggesting that the genes most affected by CR and those associated with genetic fitness are largely distinct. The cluster separation by line in the PCA plot for CR genes suggests a potential interaction effect between CR (PC1, 33.3%) and line (PC2, 11.6%).

An interaction term model was used in the determination of pathways up- and down-regulated by line and by CR. Comparison of HCR-associated biological pathways in muscle in AL and CR groups confirm the upregulation of previously described [38] KEGG pathways related to mitochondrial metabolism in HCR, including *Oxidative phosphorylation* and *Valine, leucine, and isoleucine degradation* (Figure 4A). These pathways remain upregulated after CR, likely reflecting the selection for mitochondrial gene expression during the breeding for running distance. Pathways regulated by CR in HCR and LCR muscle were similar, with the *Ribosome* pathway showing the most robust upregulation in both HCR and LCR (Figure 4B, $OR_{HCR} = 10.49$ and $OR_{LCR} = 8.66$). LCR-CR show downregulation of mitochondrial metabolic pathways including *Oxidative phosphorylation* and *Citrate cycle* that was not experienced by HCR-CR (Figure 4B). This supports the evidence suggesting that upregulation of these pathways in HCR at baseline (Figure 4A) is genetically fixed.

In the liver, PCA analysis on all genes showed clustering by line (PC1, 15.6%) and CR (PC2, 14.0%) (Figure 3D). Similar to what was observed in muscle, the genes significantly differentially expressed by line and CR in muscle were distinct (Fig. S9B). When CR main effect genes were plotted by PCA, we saw the expected clustering by CR (PC1, 56.8%) as well as line (PC2, 9.5%) (Figure 3E and F). Unlike in muscle, the pathways regulated by CR in liver differed between lines (Figure 4D). LCR showed significant (FDR <0.05) upregulation of pathways related to amino acid metabolism including *Tyrosine metabolism* and *Phenylalanine metabolism*, whereas HCR showed upregulation of pathways related to fatty acid metabolism including *C. cycle* and *Oxidative phosphorylation*. Pathways regulated by line in liver differed at baseline and with CR but were not highly significantly (Figure 4C).

3.5. LCR under CR develop a plasma lipid profile that mirrors high-CRF phenotypes

The gene expression data in liver and muscle suggests that both HCR and LCR experience a transcriptomic response to CR, although the

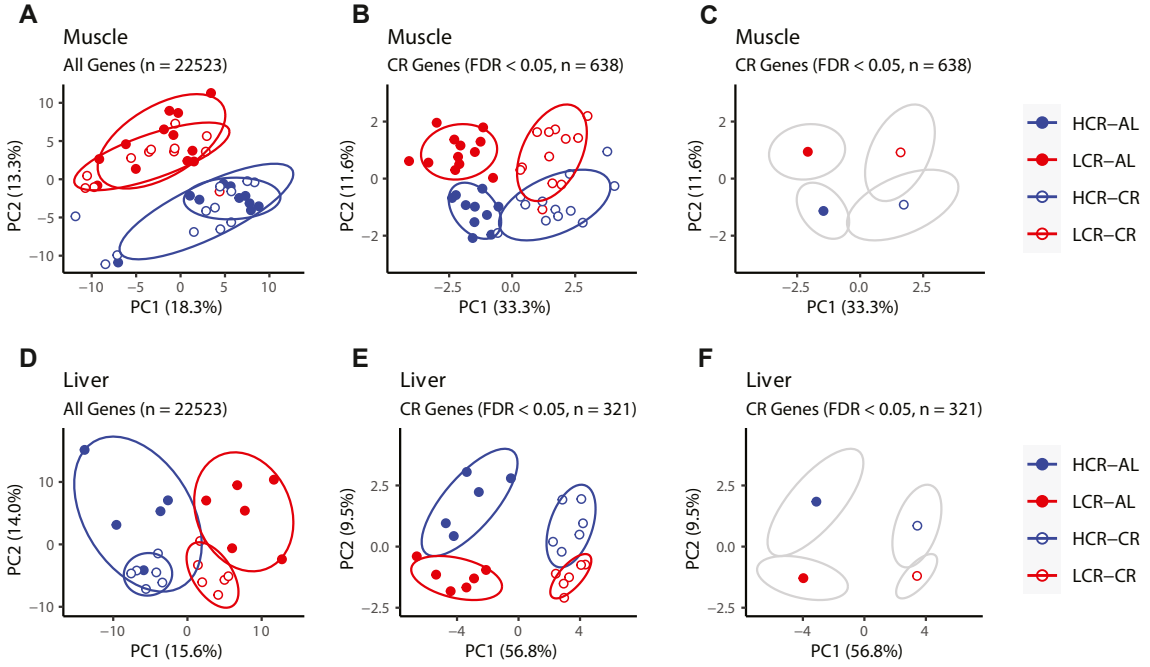

Figure 3: CR-associated regulation of gene expression in HCR and LCR is tissue dependent. PCA plots of microarray muscle gene expression data of PC1 and PC2 for all genes (A), for CR-associated genes derived from a main effect model only (B, Fig. S9A), and for CR-associated gene centroids by group (C). PCA plots of microarray liver gene expression data of PC1 and PC2 for all genes (D), for CR-associated genes derived from a main effect model only (E, Fig. S9B), and for CR-associated gene centroids by group (F). Differential gene expression data in Table S3. *HCR = high capacity runner; LCR = low capacity runner; AL = ad libitum; CR = caloric restriction.*

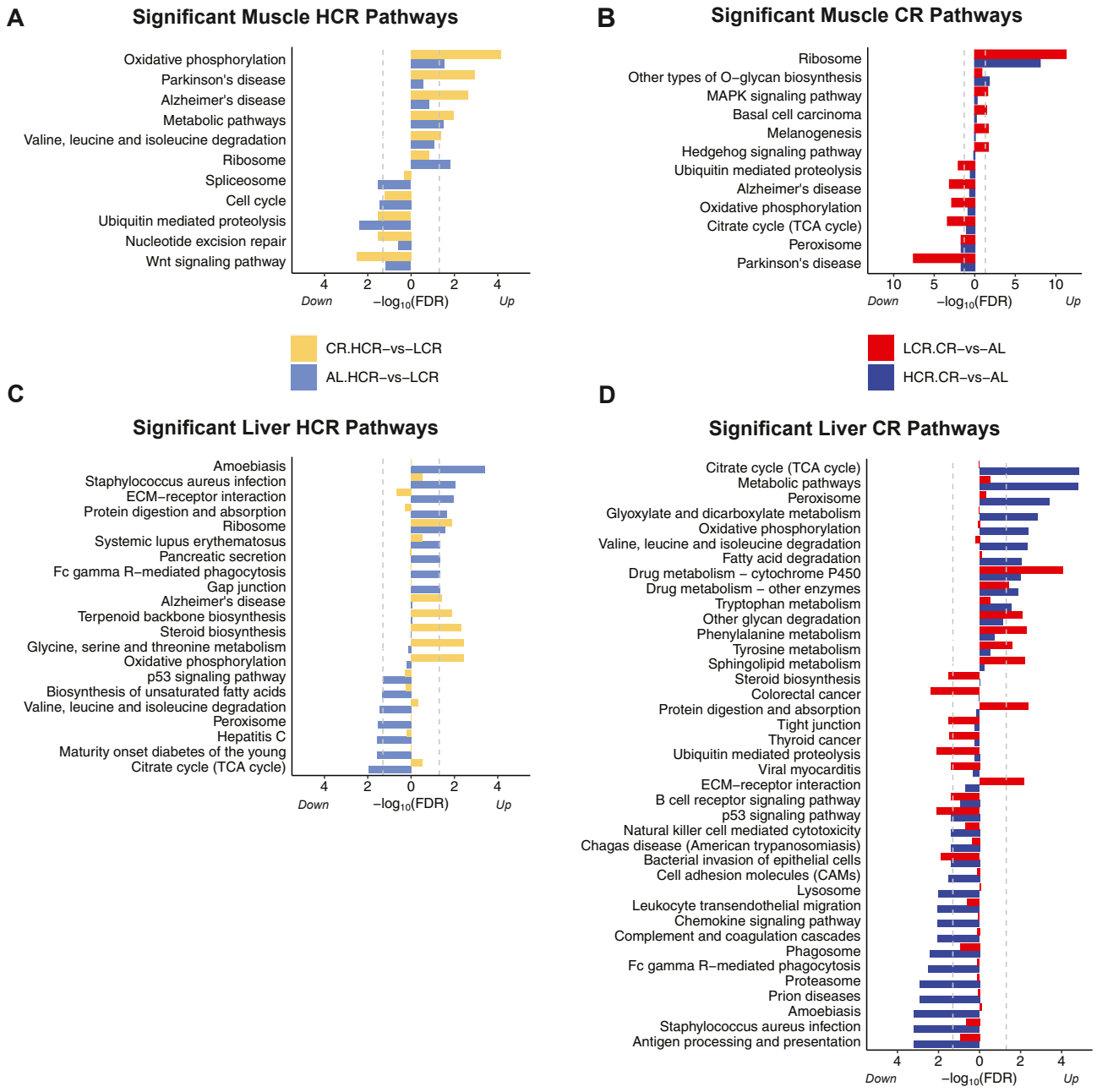

Figure 4: HCR and LCR upregulate different metabolic pathways in the liver under CR. Significant pathways are plotted by -log10(FDR) that are up-regulated (right) and down-regulated (left), in muscle by high CRF (A) or CR (B) and in liver by high CRF (C) or by CR (D). The pathways visualized have an FDR <0.05 (dotted gray line) in at least one of the comparison groups shown in each plot. Differential gene expression data in Table S3. *HCR = high capacity runner; LCR = low capacity runner; AL = ad libitum; CR = caloric restriction.*

physiologic and whole-body metabolic data suggests that this gene-level response manifests slightly differently in each line. To further observe more functional changes in metabolism with CR, lipidomic analysis was performed on the plasma of all groups at the 12-month harvest timepoint. Plasma was taken in both the fed and fasted state ("State") which was adjusted for in subsequent regression analysis. Individual lipids were categorized into clusters of like-structures (Table S4) and each cluster was quantified using multiple linear regression as a function of State, Line, Treatment, and the Treatment:Line interaction (see Methods).

The analysis indicated that LCR-AL have higher levels of plasma lipids compared to LCR-CR, HCR-CR, and HCR-AL (Figure 5A). When observing the normalized beta coefficients of each lipid cluster as a function of line and treatment, LCR-CR (captured by the interaction term, orange bars) exhibited negative beta-coefficients for many lipids clusters (Figure 5B and C), which indicates that the normalized lipid values for LCR-CR are closer to that of HCR than LCR-AL. The CR effect in LCR (Figure 5B, orange bars) reflects the results observed in other clinical variables, including body composition and insulin sensitivity (Figure 1F, G, 1H). This effect was especially significant for

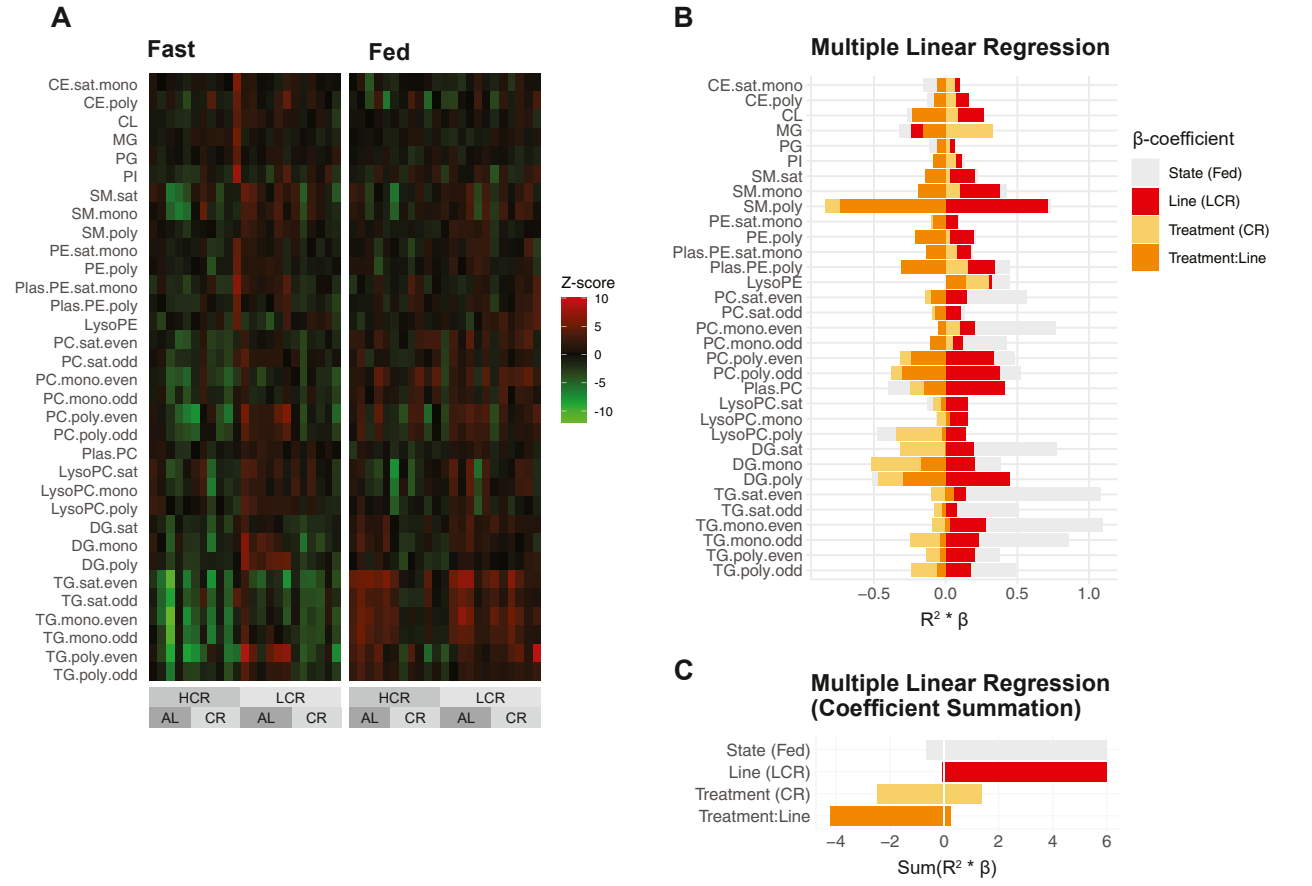

Figure 5: LCR under CR develop a plasma lipid profile that mirrors high-CRF phenotypes. Z-score normalized log2 lipidomics peak area for lipid clusters from animals in the fed and fast state show higher peak levels in LCR-AL (A). Beta coefficients from multiple linear regression analysis on lipid clusters are visualized as a function of State, Line, Treatment, and Treatment:Line (B). Beta coefficients of all lipid clusters are summed by covariate (C). Lipid clusters defined in Table S4. Statistics provided in Table S5. *HCR = high capacity runner; LCR = low capacity runner; AL = ad libitum; CR = caloric restriction.*

polyunsaturated lipids, including *polyunsaturated sphingomyelins* ($p = 0.001$, $\beta_{LCR:CR} = -1.53$, Table S5) and *polyunsaturated plasmenyl-phosphatidylethanolamines* ($p = 0.008$, $\beta_{LCR:CR} = -1.53$, Table S5), indicating that CR reduced the normally higher levels of polyunsaturated lipids in LCR compared to HCR. In the AL state and in LCR, lipid cluster values were primarily positive and significant for polyunsaturated fatty acids (Figure 5C, Table S5, grey and red bars), while CR treatment and the LCR-CR interaction resulted in lipid clusters value being negative, representing a decrease in lipid levels with CR which was more robust in the LCR (Figure 5C, yellow and orange bars).

4. DISCUSSION

This study aimed to better understand the commonalities and differences that contribute to the similar high fitness and caloric restricted phenotype, including improved metabolic health markers, leanness, and longer lifespan. Broadly, evaluation of physiological phenotypes in both lines indicate that LCR-CR experience a health-associated positive effect on body composition (Figure 1F and G), insulin sensitivity (Figure 1H), and plasma lipids (Figure 5), whose parameters strongly resemble HCR [39,40]. Examination of modeled body weight- and activity-adjusted EE ("innate" EE) shows that under CR, HCR experience a greater decrease in innate EE (Figure 2D) compared to LCR, suggesting that EE is differentially modifiable by CR in both lines. In addition, the transcriptomic results in skeletal muscle show that line-dependent gene expression is maintained after CR. Together, the results suggest that in addition to selection for fitness, the HCR line is also selected for traits associated with CR, including reduced body weight and longevity. However, HCR and LCR show some line-dependent responses to CR that are accreditable to difference in genetic makeup. The results do not support that high fitness is perceived molecularly as CR, but they do not preclude the possibility that CRF and CR pathways may converge.

Our study shows that divergent selection for running capacity appears to select for VO_2max, spontaneous activity, and innate EE. Studies showing associations between these factors are limited and the findings varied. In mice, generational selection for maximal swim time [41] or voluntary wheel running [42] resulted in elevated metabolic rate as assessed by respirometry during the inactive period. In the bank vole, VO_2max swim times elicited at 30 °C, but not 20 °C, were associated with elevated metabolic rate [43,44]. In rats, longer voluntary wheel running times caused an increased VO_2max [45] although contributions of spontaneous activity to VO_2max in the untrained state are unclear. In human data, spontaneous physical activity was not associated with VO_2max although positive associations between resting metabolic rate and VO_2max were detected [46–48]. Decreased weight and fat-free mass,

which is highly correlated with VO_2max, is associated with higher non-exercise activity thermogenesis [49].

In our data, higher CRF is associated with higher spontaneous activity (Figure 2A) and a trend towards higher innate EE (Figure 2D) likely due to the genetic selection used to generate the HCR and LCR animals, which is more robust between lines in the AL than the CR groups. A recent meta-analysis in humans has suggested an inverse genetic association between physical inactivity and fitness [24] paralleling our results that spontaneous activity and intrinsic fitness are genetically linked. Previous metabolic studies are limited in their ability to account for the many variables contributing to total EE due to difficulties collecting adequate data or limited assumptions made during analysis [50,51]. To parse innate EE differences between high and low CRF that may be separate from spontaneous activity, we took a systematic approach that incorporates body weight and cage activity, as HCR have repeatedly shown elevated activity [33,35,40,52]. Here, hourly activity counts paired with body weight-adjusted EE over repeated days at two timepoints allowed for a more thorough investigation of innate EE as it relates to fitness.

Under CR conditions, modeled innate EE decreased more in the HCR than the LCR (Figure 2D). Quantification of innate and resting EE can be further observed by summarizing the collective intercepts of the $EE_{BW-adj} \sim Activity$ models (Fig. S4), used in the adjustment analysis, under the interpretation that the intercept represents the body weight-adjusted EE of each animal given an activity level of zero (resting EE). Each animal is characterized by 5 days of data, and although the slope of the $EE_{BW-adj} \sim Activity$ model for each animal varied by day depending on activity levels, it is important to note that the intercepts of these models are consistent between days for each animal. This supports the use of the mean intercept for each animal as representation of resting EE. Collectively, HCR have significantly higher intercepts than LCR ($p < 0.001$ for Line effect), although this difference is reduced under CR (Fig. S5), suggesting a higher resting EE in HCR compared to LCR. In contrast, both lines showed a pattern of increased activity (Figure 2E) and FAO (Figure 2G) in anticipation of feeding in CR groups, underlining commonalities in their metabolic CR response.

Potentially higher resting or innate EE via thermogenesis, in addition to higher spontaneous cage activity, provides a mechanism by which HCR weigh less than their LCR counterparts. In both this study and short-term CR studies, CR attenuated weight gain equivalently in HCR and LCR (Figure 1C) while eating as much food per gram body weight, consistent with previous studies [53], highlighting the genetic selection of EE in HCR compared to LCR. Earlier CR studies in HCR and LCR support the finding that non-resting EE is suppressed by CR to a greater degree in HCR than LCR [33] where contributions from activity are accounted for by separating EE data into resting and non-resting EE as defined by physical activity counts. It is important to highlight that metabolic adaptations in rats under CR appear mechanistically different between acute [22] and chronic [23] studies and should be considered when examining CR initiated at weaning versus CR initiated after development. We also note differences in weight gain in HCR and LCR when animals were fed a highly palatable, high fat diet [35]. In this high fat diet study, high fat diet reduced spontaneous activity in both lines, suggesting that the reduction in fuel economy in the HCR line persisted under conditions of caloric overload.

Our findings show no difference in temperature between lines (Fig. S1C), lower normalized BAT weight in HCR (Table S1, $p = 0.011$ for Line effect), no difference in thyroxine (free T4) between lines (Table S1), and no difference in fecal energy content (Fig. S1B) suggesting that the differences in innate EE are not related to differences in food absorption and may be accreditable to subtle differences in the thermic effect of food and thermogenesis. We note that previous studies have differing findings. A previous study found significantly higher BAT weight and rectal temperatures in HCR compared to LCR [34]. Other studies show increased levels of uncoupling protein UCP1 in BAT of HCR [54], while others have shown no difference in UCP1 in BAT [19] which we also see in our lab (unpublished). We suspect variability in our results compared to other studies may be due to environmental housing differences such as temperature, humidity, or social housing.

Line-dependent differences in muscle gene expression under CR shows greater changes in LCR-CR than HCR-CR compared to their respective AL controls. Similar to our data, life-long CR studies have shown that *protein synthesis and turnover* and *synthesis of fatty acids and nucleotide precursors* categories are changed by CR [58] although the effect of CR on muscle gene expression in mammals is varied and sometimes contradictory [57]. Other long-term CR studies have shown the down-regulation of genes associated with energy metabolism and oxidative phosphorylation in the skeletal muscle of middle-aged rhesus monkeys [59] supporting the pathway changes observed in these studies.

In the liver, the only common pathways significantly regulated by CR in both HCR and LCR were *Drug metabolism* pathways (Figure 4D) which is a previously reported response in the liver of rats under CR [55]. In AL rats, pathway analysis indicates that fatty acid metabolism in the liver is not significantly different between HCR and LCR (Figure 4C), although HCR-CR showed an upregulation of many *Metabolism*-related pathways in liver which were not significantly changed in LCR-CR (Figure 4D). This suggests that HCR do not exhibit a CR molecular phenotype at baseline in the liver but potentially require an increase in fatty acid oxidation and oxidative phosphorylation metabolism to meet their energy needs. Increases in fatty acid oxidative pathways have been observed in rat liver under CR previously [56,57], suggesting that HCR can elicit a characteristic CR response in the liver. The decrease in innate EE in HCR under CR (Figure 2D), paired with the upregulated metabolic processes in the HCR liver (Figure 4D), may reflect a multi-pathway effort to increase the metabolite and nutrient pool under CR conditions.

This study has some limitations. The study was performed in male rats only, and investigation into the CR response in female rats would support the findings herein. However, female HCR and LCR show similar divergence in weight [14], longevity [20], and spontaneous activity [19] compared to males, suggesting that a similar line-dependent response would be observed. In our metabolic cage modeling, we were unable to directly measure and adjust for the thermic effect of food or obtain body surface area or temperature measurements, for which differences have been observed in HCR and LCR in other studies [34]. Activity measurements were obtained from metabolic cages, and the initial adjustment period to the new environment often results in an increase in activity. As our analysis focused on activity-adjusted measurements, this limitation was not considered restrictive. We did note reduced activity with each day in the metabolic cages (Figure 2A), but the differences in activity and overall EE between groups largely persisted across each time point. Our CR protocol also resulted in a time-restricted feeding (TRF) paradigm, as CR groups were fed once daily, and the rats consumed most of their food within a few hours. Studies in obese humans have indicated no difference in weight loss between CR and TRF [60] and comparative studies in mice have also indicated that improved health markers with fasting are due to CR [61]. Running protocols took place in the morning, and we were unable to control for differences in fasting times between CR and AL animals. Finally, longevity data under CR in HCR and LCR would inform the results but are beyond the scope of this study.

Our results suggest that high CRF and CR have similar metabolic and longevity phenotypes but are associated with distinct changes in

behavior and metabolism, suggesting different upstream factors that result in metabolic health and longevity. Studies observing the intersection of VO_2max and CR in humans is limited, but the phenotypes are similar. In humans, CR studies show a decline in body weight, metabolic rate, blood pressure, blood glucose, insulin, and atherosclerosis risk [62–66]; and high CRF is associated with leanness and lower rates of obesity [11], lower rates of cardiometabolic disease [12], and a significantly lower age-adjusted and disease-adjusted mortality rates [67]. Recent meta-analysis indicating an inverse genetic association between sedentary activity and fitness [24] further support the translatability of the HCR and LCR rats to humans.

FUNDING

This work was supported by National Institutes of Health RO1 DK-099034 and F31 DK-130253, the Michigan Nutrition Obesity Research Center (P30DK- 089503), and the A. Alfred Taubman Medical Research Institute.

AUTHOR CONTRIBUTIONS

Conceptualization, Methodology, Project Administration, and Funding Acquisition, N.Q., M.K.T. and C.F.B; Formal Analysis, J.Y.F., J.Z.L., N.Q. and CFB; Investigation, N.Q. and M.K.T.; Resources, N.Q., S.L.B., L.G.K, and C.F.B.; Data Curation, J.Y.F., N.Q., and M.K.T.; Writing – Original Draft, J.Y.F. and C.F.B.; Writing – Review and Editing, J.Y.F., J.Z.L., N.Q., and C.F.B.; Visualization, J.Y.F.; Supervision, N.Q. and C.F.B.

CONFLICT OF INTEREST

None declared.

DATA AVAILABILITY

Data is shared on Mendeley and as Supplementary Tables.

ACKNOWLEDGEMENTS

We thank the staff of the Michigan Mouse Metabolic Phenotyping Center for their dedicated and careful work.

APPENDIX A. SUPPLEMENTARY DATA

Supplementary data to this article can be found online at https://doi.org/10.1016/j.molmet.2023.101668.

REFERENCES

[1] Houthoofd K, Braeckman BP, Lenaerts I, Brys K, De Vreese A, Van Eygen S, et al. Axenic growth up-regulates mass-specific metabolic rate, stress resistance, and extends life span in Caenorhabditis elegans. Exp Gerontol 2002;37(12):1371–8.

[2] Pletcher SD, Macdonald SJ, Marguerie R, Certa U, Stearns SC, Goldstein DB, et al. Genome-wide transcript profiles in aging and calorically restricted Drosophila melanogaster. Curr Biol : CB 2002;12(9):712–23.

[3] Weindruch R, Walford RL, Fligiel S, Guthrie D. The retardation of aging in mice by dietary restriction: longevity, cancer, immunity and lifetime energy intake. J Nutr 1986;116(4):641–54.

[4] McCay CM, Crowell MF, Maynard LA. The effect of retarded growth upon the length of life span and upon the ultimate body size: one figure. J Nutr 1935;10(1):63–79.

[5] Bodkin NL, Alexander TM, Ortmeyer HK, Johnson E, Hansen BC. Mortality and morbidity in laboratory-maintained Rhesus monkeys and effects of long-term dietary restriction. The journals of gerontology. Series A, Biological sciences and medical sciences 2003;58(3):212–9.

[6] Redman LM, Ravussin E. Caloric restriction in humans: impact on physiological, psychological, and behavioral outcomes. Antioxidants Redox Signal 2011;14(2):275–87.

[7] Collins N, Belkaid Y. Control of immunity via nutritional interventions. Immunity 2022;55(2):210–23.

[8] Heilbronn LK, de Jonge L, Frisard MI, DeLany JP, Larson-Meyer DE, Rood J, et al. Effect of 6-month calorie restriction on biomarkers of longevity, metabolic adaptation, and oxidative stress in overweight individuals: a randomized controlled trial. JAMA 2006;295(13):1539–48.

[9] Green CL, Lamming DW, Fontana L. Molecular mechanisms of dietary restriction promoting health and longevity. Nat Rev Mol Cell Biol 2022;23(1):56–73.

[10] Schutte NM, Nederend I, Hudziak JJ, Bartels M, de Geus EJ. Twin-sibling study and meta-analysis on the heritability of maximal oxygen consumption. Physiol Genom 2016;48(3):210–9.

[11] Ortega R, Grandes G, Sanchez A, Montoya I, Torcal J. Cardiorespiratory fitness and development of abdominal obesity. Prev Med 2019;118:232–7.

[12] Clausen JSR, Marott JL, Holtermann A, Gyntelberg F, Jensen MT. Midlife cardiorespiratory fitness and the long-term risk of mortality: 46 Years of follow-up. J Am Coll Cardiol 2018;72(9):987–95.

[13] Strasser B, Burtscher M. Survival of the fittest: VO2max, a key predictor of longevity. Front Biosci (Online) 2018;23(8):1505–16.

[14] Koch LG, Britton SL. Artificial selection for intrinsic aerobic endurance running capacity in rats. Physiol Genom 2001;5(1):45–52.

[15] Wisløff U, Najjar SM, Ellingsen O, Haram PM, Swoap S, Al-Share Q, et al. Cardiovascular risk factors emerge after artificial selection for low aerobic capacity. Science (New York, N.Y.) 2005;307(5708):418–20.

[16] Overmyer KA, Evans CR, Qi NR, Minogue CE, Carson JJ, Chermside-Scabbo CJ, et al. Maximal oxidative capacity during exercise is associated with skeletal muscle fuel selection and dynamic changes in mitochondrial protein acetylation. Cell Metabol 2015;21(3):468–78.

[17] Gavini CK, Mukherjee S, Shukla C, Britton SL, Koch LG, Shi H, et al. Leanness and heightened nonresting energy expenditure: role of skeletal muscle activity thermogenesis. Am J Physiol Endocrinol Metab 2014;306(6):E635–47.

[18] Morris EM, Meers GME, Ruegsegger GN, Wankhade UD, Robinson T, Koch LG, et al. Intrinsic high aerobic capacity in male rats protects against diet-induced insulin resistance. Endocrinology 2019;160(5):1179–92.

[19] Vieira-Potter VJ, Padilla J, Park YM, Welly RJ, Scroggins RJ, Britton SL, et al. Female rats selectively bred for high intrinsic aerobic fitness are protected from ovariectomy-associated metabolic dysfunction. Am J Physiol Regul Integr Comp Physiol 2015;308(6):R530–42.

[20] Koch LG, Kemi OJ, Qi N, Leng SX, Bijma P, Gilligan LJ, et al. Intrinsic aerobic capacity sets a divide for aging and longevity. Circ Res 2011;109(10):1162–72.

[21] Forsum E, Hillman PE, Nesheim MC. Effect of energy restriction on total heat production, basal metabolic rate, and specific dynamic action of food in rats. J Nutr 1981;111(10):1691–7.

[22] Khan MA, Bender AE. Adaptation to restricted intake of protein and energy. Nutr Metabol 1979;23(6):449–57.

[23] Mohan PF, Rao BS. Adaptation to underfeeding in growing rats. Effect of energy restriction at two dietary protein levels on growth, feed efficiency, basal metabolism and body composition. J Nutr 1983;113(1):79–85.

[24] Wang Z, Emmerich A, Pillon NJ, Moore T, Hemerich D, Cornelis MC, et al. Genome-wide association analyses of physical activity and sedentary behavior provide insights into underlying mechanisms and roles in disease prevention. Nat Genet 2022;54(9):1332–44.

[25] Péronnet F, Massicotte D. Table of nonprotein respiratory quotient: an update. Canadian journal of sport sciences = Journal canadien des sciences du sport 1991;16(1):23–9.
[26] Simonson DC, DeFronzo RA. Indirect calorimetry: methodological and interpretative problems. Am J Physiol 1990;258(3 Pt 1):E399–412.
[27] Frayn KN. Calculation of substrate oxidation rates in vivo from gaseous exchange. J Appl Physiol Respir Environ Exerc Physiol 1983;55(2):628–34.
[28] Ferrannini E. The theoretical bases of indirect calorimetry: a review. Metab Clin Exp 1988;37(3):287–301.
[29] Kim JH, Karnovsky A, Mahavisno V, Weymouth T, Pande M, Dolinoy DC, et al. LRpath analysis reveals common pathways dysregulated via DNA methylation across cancer types. BMC Genom 2012;13:526.
[30] LaBarre JL, Puttabyatappa M, Song PXK, Goodrich JM, Zhou L, Rajendiran TM, et al. Maternal lipid levels across pregnancy impact the umbilical cord blood lipidome and infant birth weight. Sci Rep 2020;10(1):14209.
[31] Fernández-Verdejo R, Aguirre C, Galgani JE. Issues in measuring and interpreting energy balance and its contribution to obesity. Current obesity reports 2019;8(2):88–97.
[32] Ferraro R, Ravussin E. Fat mass in predicting resting metabolic rate. Am J Clin Nutr 1992;56(2):460–1.
[33] Mukherjee SD, Koch LG, Britton SL, Novak CM. Aerobic capacity modulates adaptive thermogenesis: contribution of non-resting energy expenditure. Physiol Behav 2020;225:113048.
[34] Karvinen SM, Silvennoinen M, Ma H, Törmäkangas T, Rantalainen T, Rinnankoski-Tuikka R, et al. Voluntary running aids to maintain high body temperature in rats bred for high aerobic capacity. Front Physiol 2016;7:311.
[35] Novak CM, Escande C, Burghardt PR, Zhang M, Barbosa MT, Chini EN, et al. Spontaneous activity, economy of activity, and resistance to diet-induced obesity in rats bred for high intrinsic aerobic capacity. Horm Behav 2010;58(3):355–67.
[36] DeMarco VG, Johnson MS, Ma L, Pulakat L, Mugerfeld I, Hayden MR, et al. Overweight female rats selectively breed for low aerobic capacity exhibit increased myocardial fibrosis and diastolic dysfunction. Am J Physiol Heart Circ Physiol 2012;302(8):H1667–82.
[37] Bruss MD, Khambatta CF, Ruby MA, Aggarwal I, Hellerstein MK. Calorie restriction increases fatty acid synthesis and whole body fat oxidation rates. Am J Physiol Endocrinol Metab 2010;298(1):E108–16.
[38] Ren YY, Koch LG, Britton SL, Qi NR, Treutelaar MK, Burant CF, et al. Selection-, age-, and exercise-dependence of skeletal muscle gene expression patterns in a rat model of metabolic fitness. Physiol Genom 2016;48(11):816–25.
[39] Bowman TA, Ramakrishnan SK, Kaw M, Lee SJ, Patel PR, Golla VK, et al. Caloric restriction reverses hepatic insulin resistance and steatosis in rats with low aerobic capacity. Endocrinology 2010;151(11):5157–64.
[40] Smyers ME, Koch LG, Britton SL, Wagner JG, Novak CM. Enhanced weight and fat loss from long-term intermittent fasting in obesity-prone, low-fitness rats. Physiol Behav 2021;230:113280.
[41] Gebczyński AK, Konarzewski M. Metabolic correlates of selection on aerobic capacity in laboratory mice: a test of the model for the evolution of endothermy. J Exp Biol 2009;212(17):2872–8.
[42] Kane SL, Garland T, Carter PA. Basal metabolic rate of aged mice is affected by random genetic drift but not by selective breeding for high early-age locomotor activity or chronic wheel access. Physiol Biochem Zool: PBZ 2008;81(3):288–300.
[43] Sadowska ET, Labocha MK, Baliga K, Stanisz A, Wróblewska AK, Jagusiak W, et al. Genetic correlations between basal and maximum metabolic rates in a wild rodent: consequences for evolution of endothermy. Evolution 2005;59(3):672–81.
[44] Sadowska ET. Evolution of metabolic rate: heritability, genetic correlations and effects of artificial selection in the bank vole (Clethrionomys glareolus). PhD Thesis. Jagiellon University; 2008 [in Polish)].
[45] Lambert MI, Noakes TD. Spontaneous running increases VO2max and running performance in rats. J Appl Physiol 1990;68(1):400–3 (1985).
[46] Ando T, Piaggi P, Bogardus C, Krakoff J. VO2max is associated with measures of energy expenditure in sedentary condition but does not predict weight change. Metab Clin Exp 2019;90:44–51.
[47] Tangen EM, Gjestvang C, Stensrud T, Haakstad LAH. Is there an association between total physical activity level and VO2max among fitness club members? A cross-sectional study. BMC Sports Sci Med Rehabil 2022;14(1):109.
[48] Ebaditabar M, Imani H, Babaei N, Davarzani S, Shab-Bidar S. Maximal oxygen consumption is positively associated with resting metabolic rate and better body composition profile. Obesity medicine 2020;2451–8476(21). https://doi.org/10.1016/j.obmed.2020.100309.
[49] Levine JA. Nonexercise activity thermogenesis–liberating the life-force. J Intern Med 2007;262(3):273–87.
[50] Speakman JR. Measuring energy metabolism in the mouse - theoretical, practical, and analytical considerations. Front Physiol 2013;4:34.
[51] Müller TD, Klingenspor M, Tschöp MH. Revisiting energy expenditure: how to correct mouse metabolic rate for body mass. Nature metabolism 2021;3(9):1134–6.
[52] Smyers ME, Bachir KZ, Britton SL, Koch LG, Novak CM. Physically active rats lose more weight during calorie restriction. Physiol Behav 2015;139:303–13.
[53] Davis AE, Smyers ME, Beltz L, Mehta DM, Britton SL, Koch LG, et al. Differential weight loss with intermittent fasting or daily calorie restriction in low- and high-fitness phenotypes. Exp Physiol 2021;106(8):1731–42.
[54] Matthew Morris E, Meers GM, Koch LG, Britton SL, MacLean PS, Thyfault JP. Increased aerobic capacity reduces susceptibility to acute high-fat diet-induced weight gain. Obesity (Silver Spring, Md 2016;24(9):1929–37.
[55] Leakey JE, Cunny HC, Bazare J, Webb PJ, Feuers RJ, Duffy PH, et al. Effects of aging and caloric restriction on hepatic drug metabolizing enzymes in the Fischer 344 rat. I: the cytochrome P-450 dependent monooxygenase system. Mechanisms of ageing and development 1989;48(2):145–55.
[56] Saito K, Ohta Y, Sami M, Kanda T, Kato H. Effect of mild restriction of food intake on gene expression profile in the liver of young rats: reference data for in vivo nutrigenomics study. Br J Nutr 2010;104(7):941–50.
[57] Swindell WR. Genes and gene expression modules associated with caloric restriction and aging in the laboratory mouse. BMC Genom 2009;10:585.
[58] Lee CK, Klopp RG, Weindruch R, Prolla TA. Gene expression profile of aging and its retardation by caloric restriction. Science (New York, N.Y.) 1999;285(5432):1390–3.
[59] Kayo T, Allison DB, Weindruch R, Prolla TA. Influences of aging and caloric restriction on the transcriptional profile of skeletal muscle from rhesus monkeys. Proc Natl Acad Sci U S A 2001;98(9):5093–8.
[60] Liu D, Huang Y, Huang C, Yang S, Wei X, Zhang P, et al. Calorie restriction with or without time-restricted eating in weight loss. N Engl J Med 2022;386(16):1495–504.
[61] Henderson CG, Turner DL, Swoap SJ. Health effects of alternate day fasting versus pair-fed caloric restriction in diet-induced obese C57Bl/6J male mice. Front Physiol 2021;12:641532.
[62] Weyer C, Walford RL, Harper IT, Milner M, MacCallum T, Tataranni PA, et al. Energy metabolism after 2 y of energy restriction: the biosphere 2 experiment. Am J Clin Nutr 2000;72(4):946–53.
[63] Walford RL, Harris SB, Gunion MW. The calorically restricted low-fat nutrient-dense diet in Biosphere 2 significantly lowers blood glucose, total leukocyte count, cholesterol, and blood pressure in humans. Proc Natl Acad Sci U S A 1992;89(23):11533–7.
[64] Walford RL, Mock D, Verdery R, MacCallum T. Calorie restriction in biosphere 2: alterations in physiologic, hematologic, hormonal, and biochemical parameters in humans restricted for a 2-year period. The journals of

gerontology. Series A, Biological sciences and medical sciences 2002;57(6): B211–24.

[65] Walford RL, Mock D, MacCallum T, Laseter JL. Physiologic changes in humans subjected to severe, selective calorie restriction for two years in biosphere 2: health, aging, and toxicological perspectives. Toxicol Sci : An Official Journal of the Society of Toxicology 1999;52(2 Suppl):61–5.

[66] Fontana L, Meyer TE, Klein S, Holloszy JO. Long-term calorie restriction is highly effective in reducing the risk for atherosclerosis in humans. Proc Natl Acad Sci U S A 2004;101(17):6659–63.

[67] Sawada SS, Lee IM, Muto T, Matuszaki K, Blair SN. Cardiorespiratory fitness and the incidence of type 2 diabetes: prospective study of Japanese men. Diabetes Care 2003;26(10):2918–22.

